Published in final edited form as:
Science. 2013 April 19; 340(6130): 356–359. doi:10.1126/science.1234264.

Structural Basis For Kinesin-1:Cargo Recognition

Stefano Pernigo[1], **Anneri Lamprecht**[1], **Roberto A. Steiner**[*], and **Mark P. Dodding**[*]
Randall Division of Cell and Molecular Biophysics, King's College London, SE1 1UL, UK.

Abstract

Kinesin-mediated cargo transport is required for many cellular functions and plays a key role in pathological processes. Structural information on how kinesins recognize their cargoes is required for a molecular understanding of this fundamental and ubiquitous process. Here we present the crystal structure of the tetratricopeptide repeat of kinesin light chain 2 in complex with a cargo peptide harboring a 'tryptophan-acidic' motif derived from SKIP, a critical host determinant in *Salmonella* pathogenesis and a regulator of lysosomal positioning. Structural data together with biophysical, biochemical and cellular assays allow us to propose a framework for intracellular transport based on the binding by kinesin-1 of W-acidic cargo motifs through a combination of electrostatic interactions and sequence-specific elements, providing direct molecular evidence of the mechanisms for kinesin-1:cargo recognition.

The plus-end directed motor, kinesin-1 plays a critical role in the intracellular transport of diverse protein, ribonuclear protein complexes and membrane compartments on microtubules (1). Its functions are also usurped by bacteria and viruses to aid in their replication (2, 3). Kinesin-1 can perform this diverse range of functions by virtue of its ability to interact with many different cargo proteins (4). Diversity of cargo recognition is accomplished largely through the kinesin light chains (KLC) which harbour a tetratricopeptide repeat (TPR) domain, a versatile protein interaction platform (5, 6). The KLC^{TPR} domain can recognise short peptide stretches within relatively disordered regions of its targets. These peptides are characterized by a tryptophan residue flanked by acidic residues (e.g. EWD) and are found in a growing list of KLC binding proteins (7-16). Although W-acidic motifs often occur in pairs, single motifs are also functional and can support microtubule-based transport even when explanted from their host protein (7, 12, 17). We set out to solve the structure of a KLC^{TPR} domain bound to a cargo W-acidic motif. We focused our attention on the SKIP cargo for its importance in *Salmonella* pathogenesis. SKIP contains a pair of W-acidic motifs centred at amino acid positions 207-208 (WD) and 236-237 (WE) that fall within the N-terminal kinesin-1 binding region (residues 1-310)(3, 7, 13) (Fig. 1A). To assess the relative importance of the SKIP W-acidic motifs for KLC binding we co-transfected HeLa cells with wild-type and WD/WE mutant constructs expressing GFP-SKIP(1-310) and HA-KLC2 (Fig. 1B). Disruption of the WD motif significantly reduced GFP-SKIP interaction with HA-KLC2 whereas abrogation of the WE motif had no obvious effects. A double mutant with both motifs disrupted displayed HA-KLC2 binding similar to the single WD mutant. Thus the WE motif has a very low affinity for KLC2. Indeed, a ten amino acid long peptide centered on the WD motif ($SKIP^{WD}$, Figure 1A) bound to $KLC2^{TPR}$ with a K_D of 24 μM whereas the affinity of the equivalent $SKIP^{WE}$ peptide was above 110 μM (Fig. 1C). The presence of both motifs improves the affinity for $KLC2^{TPR}$ because a 40 amino acid long peptide $SKIP^{WDWE}$ which encompasses

[*]To whom correspondence should be addressed. mark.dodding@kcl.ac.uk, roberto.steiner@kcl.ac.uk.
[1]These authors contributed equally to this work

The authors declare no competing financial interests.

Europe PMC Funders Author Manuscripts

the W-acid pair sequence bound with an apparent affinity higher than that of the single SKIP^{WD} motif (K_D = 4.9 μM). Binding affinity measurements at varying NaCl concentrations showed that electrostatic interactions play an important role in the recognition process (Fig. S1). For structural studies we focused on the SKIP^{WD} motif and to facilitate the crystallization process, we engineered a chimeric construct in which the SKIP^{WD} peptide was fused N-terminal to KLC2^{TPR} via a flexible $(TGS)_4$ linker (18). Crystals of SKIP^{WD}-KLC2^{TPR} grew using vapour diffusion techniques and diffracted at 2.9 Å using synchrotron radiation. The final model of the cargo complex is characterized by R and R_{free} value of 20.3 and 24.5%, respectively (Table S1). KLC2^{TPR} consists of six TPR repeats (TPR1-6) each contributed by a classical helix-turn-helix structural motif arranged in a right-handed super-helical conformation with a non-TPR helix is positioned between TPR5 and TPR6 (14). The structure of SKIP^{WD}-KLC2^{TPR} revealed the cargo peptide bound in an extended conformation at the N-terminal portion of KLC2^{TPR} concave surface with a direction parallel to the external helix of the repeat (Fig. 2A,B and Fig. S2). Although our construct includes the external helix of TPR1, this region, as well as other flexible stretches, could not be unambiguously interpreted in the electron density. Thus, KLC2^{TPR} starts from TPR2 in our model. A comparison between apo KLC2^{TPR} (3CEQ) and cargo-bound KLC2^{TPR} revealed structural differences considered to arise from a rigid jaw movement of the N-terminal TPR2-3 region which closes upon cargo recognition engendering the binding surface and pockets for the SKIP^{WD} peptide. (Fig. 2B, S3). An analysis using the PISA algorithm (19) indicates that all residues of the SKIP^{WD} peptide are involved in formation of the complex, which is stabilized by residues from TPR2-3 and the internal helix of TPR4 (Fig. 2C). This concave groove surface displays a positive electrostatic charge ideally poised to complement the negatively charged W-acidic cargo motifs (Figure 2C and Fig. S4). Overall, the interface area of the SKIP^{WD}-KLC2^{TPR} complex is about 770 Å^2, stabilized by a mixture of H-bonds, salt bridges and hydrophobic interactions (Figure 3A). The W residue central to the motif is generally flanked by amino acids bearing a carboxylate side-chain. SKIP^{W207} (position 0, p0) is buried within a leucine-rich pocket positioned roughly in the middle along the TPR length and contributed by side-chains from TPR2 (L248, R251, L263) and TPR3 (N287, L290, L291). In particular, the side-chain of N287 is in a conformation such that it serves the dual purpose of stabilizing SKIP^{W207} indole group by lining one side of the pocket whilst engaging at the same time in hydrogen bonds with the main chain amide and carbonyl oxygen of the residue at p+1. The latter position is almost invariably occupied by a glutamic or aspartic acid residue (7). The carboxylate side-chain of SKIP^{D208} points in the opposite direction to that of SKIP^{W207} engaging in a network of salt bridges and H-bonds with the positively charged R312 and K325 side-chains of α3E and α4I, respectively. An acidic side-chain at position p−1 (SKIP^{E206}) of the motif is also very conserved in other W-acidic motifs. Like SKIP^{D208}, the carboxylate side-chain of SKIP^{E206} faces the TPR3-4 side of the KLC2^{TPR} recognition groove where it is stabilized by an ionic interaction with K325. Position p-2 of SKIP^{WD} features a leucine residue (SKIP^{L205}). The hydrophobic side chain of SKIP^{L205} is deeply buried in a hydrophobic pocket formed by residues from TPR3 and 4. The side-chain of N329 plays a similar dual role as N287. Whilst lining the SKIP^{L205} pocket it also H-bonds with the main chain at position p−1. Together, N287 and N329 act like a clamp on opposite sides of SKIP^{WD} providing four of the ten hydrogen bonds that stabilize the complex. Residues at positions p-(3,4) are less important for complex stability consistent with their general lack of sequence conservation amongst W-acidic motif cargo (7). The C-terminal stretch of SKIP^{WD} encompassing p+(2,3,4,5) is observed in a more compact, turn-like conformation with SKIP^{D209,S210} at p+(2,3) making very minor contacts with the groove. As for the N-terminal peripheral region of SKIP^{WD} the exact nature of the amino acids at p+(4,5) does not seem critical for complex stability. Alternative side-chains can be positioned at this topological position possibly involving a rearrangement of the main-chain. To investigate the effect of amino acid replacements within the KLC2^{TPR} region on the interaction with SKIP we used immunoprecipitation as described above. All

amino acid substitutions tested resulted in abrogation or near abrogation of complex formation between KLC2 and SKIP (Fig 3B,C). The importance of electrostatic interactions in cargo recognition is underscored by charge-reversal mutations (Fig 3B,C). When co-expressed in cells, SKIP and its small GTPase binding partner Arl8 associate strongly with lysosomes and promote their trafficking to the cell periphery. GFP-KLC2 associates with the same lysosomes (Fig. 3D, S5) (13). This is essentially abolished by KLC2 mutations (R251D, N287L and R312E) (Fig. 3D, S5). The same mutations strongly inhibited the binding of $KLC2^{TPR}$ to the WD motif peptide (Fig. 3C). We conclude that optimal SKIP:KLC2 stability critically depends on a very conserved cargo recognition-interaction groove. We have extended our analysis to the well characterized Calsyntenin (CSTN) cargo which also exhibits two W-acidic motifs (9, 11, 12). Differently from SKIP, both CSTN motifs bind to $KLC2^{TPR}$ with similar affinity (Fig S6). However, the mutations in the KLC2 binding groove which disrupt $SKIP^{WD}$ binding also abrogate recognition of CSTN (Fig S6). A sequence alignment shows total conservation of the KLC^{TPR} residues interacting with the cargo across the kinesin light chain family (Fig. S7). Thus, the concave groove within the TPR domain where the $SKIP^{WD}$ peptide binds is likely to be the primary site of interaction for W-acidic cargo motifs in general. However, we cannot exclude that secondary sites also exist. In the context of intracellular transport where kinesin-1 functions as a tetramer containing two KLCs held together by a coiled-coil region and both SKIP motifs contribute to transport (7, 13), it is tempting to speculate that both chains can contribute to the binding of the W-acidic cargo pair. For SKIP, the higher affinity WD motif would direct the first binding event to one of the KLC^{TPR} with avidity effect promoting the association of the WE motif to the other KLC (20, 21). It will be important to determine this relationship to the kinesin-1 tetramer and examine the importance of cargo induced TPR conformational change in motor activation.

Supplementary Material

Refer to Web version on PubMed Central for supplementary material.

Acknowledgments

Scientists of I24 beamline (Diamond Light Source, Didcot, UK) are gratefully acknowledged for their support during data collection. ARL8b-HA and myc-SKIP were a kind gift from Dr. S. Munro, (LMB-MRC, Cambridge). We thank Prof. T. Blundell (University of Cambridge) for useful discussions. Coordinates and structure factor files for have been deposited in the Protein Data Bank under accession number **3ZFW**. M.P.D and A.L. are supported by a Wellcome Trust Research Career Development Fellowship to M.P.D. and a London Law Trust Medal Fellowship to M.P.D. S.P. is supported by a British Heart Foundation grant awarded to R.A.S.

References

1. Hirokawa N, Noda Y, Tanaka Y, Niwa S. Kinesin superfamily motor proteins and intracellular transport. Nat Rev Mol Cell Biol. Oct.2009 10:682. [PubMed: 19773780]
2. Dodding MP, Way M. Coupling viruses to dynein and kinesin-1. Embo J. Aug 31.2011 30:3527. [PubMed: 21878994]
3. Boucrot E, Henry T, Borg JP, Gorvel JP, Meresse S. The intracellular fate of Salmonella depends on the recruitment of kinesin. Science. May 20.2005 308:1174. [PubMed: 15905402]
4. Gindhart JG. Towards an understanding of kinesin-1 dependent transport pathways through the study of protein-protein interactions. Brief Funct Genomic Proteomic. Mar.2006 5:74. [PubMed: 16769683]
5. D'Andrea LD, Regan L. TPR proteins: the versatile helix. Trends Biochem Sci. Dec.2003 28:655. [PubMed: 14659697]
6. Hammond JW, Griffin K, Jih GT, Stuckey J, Verhey KJ. Co-operative versus independent transport of different cargoes by Kinesin-1. Traffic. May.2008 9:725. [PubMed: 18266909]

7. Dodding MP, Mitter R, Humphries AC, Way M. A kinesin-1 binding motif in vaccinia virus that is widespread throughout the human genome. Embo J. Nov 16.2011 30:4523. [PubMed: 21915095]
8. Aoyama T, et al. Cayman ataxia protein caytaxin is transported by kinesin along neurites through binding to kinesin light chains. J Cell Sci. Nov 15.2009 122:4177. [PubMed: 19861499]
9. Konecna A, et al. Calsyntenin-1 docks vesicular cargo to kinesin-1. Mol Biol Cell. Aug.2006 17:3651. [PubMed: 16760430]
10. Schmidt MR, et al. Regulation of endosomal membrane traffic by a Gadkin/AP-1/kinesin KIF5 complex. Proc Natl Acad Sci U S A. Sep 8.2009 106:15344. [PubMed: 19706427]
11. Araki Y, et al. The novel cargo Alcadein induces vesicle association of kinesin-1 motor components and activates axonal transport. Embo J. Mar 21.2007 26:1475. [PubMed: 17332754]
12. Kawano T, et al. A small peptide sequence is sufficient for initiating kinesin-1 activation through part of TPR region of KLC1. Traffic. Jun.2012 13:834. [PubMed: 22404616]
13. Rosa-Ferreira C, Munro S. Arl8 and SKIP act together to link lysosomes to kinesin-1. Dev Cell. Dec 13.2011 21:1171. [PubMed: 22172677]
14. Zhu H, et al. Crystal structures of the tetratricopeptide repeat domains of kinesin light chains: insight into cargo recognition mechanisms. PLoS One. 2012; 7:e33943. [PubMed: 22470497]
15. McGuire JR, Rong J, Li SH, Li XJ. Interaction of Huntingtin-associated protein-1 with kinesin light chain: implications in intracellular trafficking in neurons. J Biol Chem. Feb 10.2006 281:3552. [PubMed: 16339760]
16. Ligon LA, Tokito M, Finklestein JM, Grossman FE, Holzbaur EL. A direct interaction between cytoplasmic dynein and kinesin I may coordinate motor activity. J Biol Chem. Apr 30.2004 279:19201. [PubMed: 14985359]
17. Morgan GW, et al. Vaccinia protein F12 has structural similarity to kinesin light chain and contains a motor binding motif required for virion export. PLoS Pathog. Feb.2010 6:e1000785. [PubMed: 20195521]
18. Pellegrini L, et al. Insights into DNA recombination from the structure of a RAD51-BRCA2 complex. Nature. Nov 21.2002 420:287. [PubMed: 12442171]
19. Krissinel E, Henrick K. Inference of macromolecular assemblies from crystalline state. J Mol Biol. Sep 21.2007 372:774. [PubMed: 17681537]
20. Radnai L, et al. Affinity, avidity, and kinetics of target sequence binding to LC8 dynein light chain isoforms. J Biol Chem. Dec 3.2010 285:38649. [PubMed: 20889982]
21. Mack ET, et al. Dependence of avidity on linker length for a bivalent ligand-bivalent receptor model system. Journal of the American Chemical Society. Jan 11.2012 134:333. [PubMed: 22088143]
22. Hu TC, Korczynska J, Smith DK, Brzozowski AM. High-molecular-weight polymers for protein crystallization: poly-gamma-glutamic acid-based precipitants. Acta Crystallogr D Biol Crystallogr. Sep.2008 64:957. [PubMed: 18703844]
23. Winter G. xia2: an expert system for macromolecular crystallography data reduction. Journal of Applied Crystallography. 2010; 43:186.
24. Kabsch W. Integration, scaling, space-group assignment and post-refinement. Acta Crystallographica Section D. 2010; 66:133.
25. Evans P. Scaling and assessment of data quality. Acta Crystallographica Section D. 2006; 62:72.
26. Vagin A, Teplyakov A. MOLREP: an Automated Program for Molecular Replacement. Journal of Applied Crystallography. 1997; 30:1022.
27. Steiner RA, Lebedev AA, Murshudov GN. Fisher's information in maximum-likelihood macromolecular crystallographic refinement. Acta Crystallographica Section D. 2003; 59:2114.
28. Murshudov GN, et al. REFMAC5 for the refinement of macromolecular crystal structures. Acta Crystallographica Section D. 2011; 67:355.
29. Bricogne, G., et al. BUSTER. version 2.10.0. Global Phasing Ltd; Cambridge, United Kingdom: 2011.
30. Emsley P, Cowtan K. Coot: model-building tools for molecular graphics. Acta Crystallographica Section D. 2004; 60:2126.

31. Brünger AT, et al. Crystallography & NMR System: A New Software Suite for Macromolecular Structure Determination. Acta Crystallographica Section D. 1998; 54:905.
32. Davis IW, et al. MolProbity: all-atom contacts and structure validation for proteins and nucleic acids. Nucleic Acids Res. Jul.2007 35:W375. [PubMed: 17452350]
33. Dodding MP, Newsome TP, Collinson LM, Edwards C, Way M. An E2-F12 complex is required for intracellular enveloped virus morphogenesis during vaccinia infection. Cell Microbiol. May. 2009 11:808. [PubMed: 19207726]

Europe PMC Funders Author Manuscripts

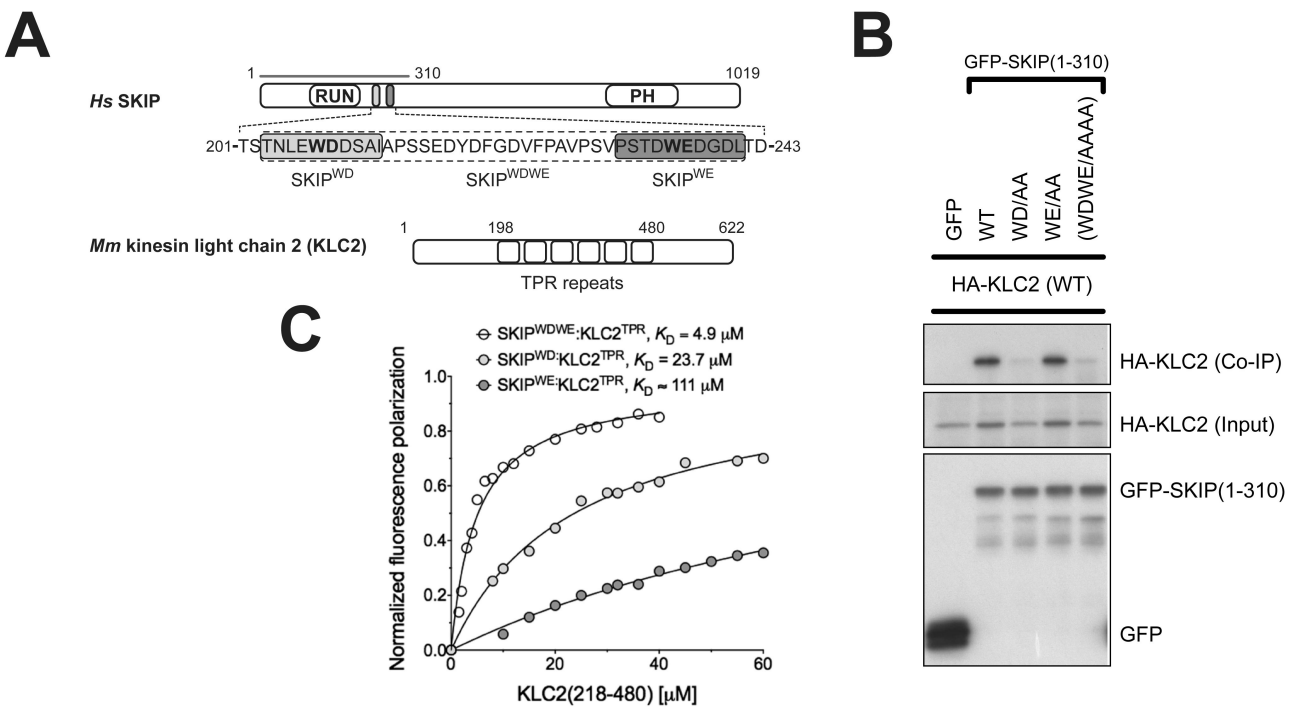

Figure 1.

Binding of SifA-kinesin binding protein (SKIP) to kinesin light chain 2 (KLC2). **(A)** Scheme of SKIP and KLC2. The two W-acidic motifs and KLC2 TPR repeats are highlighted. **(B)** Co-immunoprecipitation shows that alanine replacement in the first W-acidic motif (WD) abrogates SKIP:KLC2 binding whereas the same substitution in the second motif (WE) has virtually no effect. **(C)** Fluorescence polarization measurements confirm that the first SKIP W-acidic motif ($SKIP^{WD}$) has a higher affinity for the TPR domain of KLC2 than the second one ($SKIP^{WE}$). A peptide encompassing both motifs ($SKIP^{WDWE}$) binds with higher affinity than the best single motif. K_D values reported here were calculated at 150 mM NaCl. Binding affinity values at varying ionic strength values are given in Fig. S1.

Europe PMC Funders Author Manuscripts

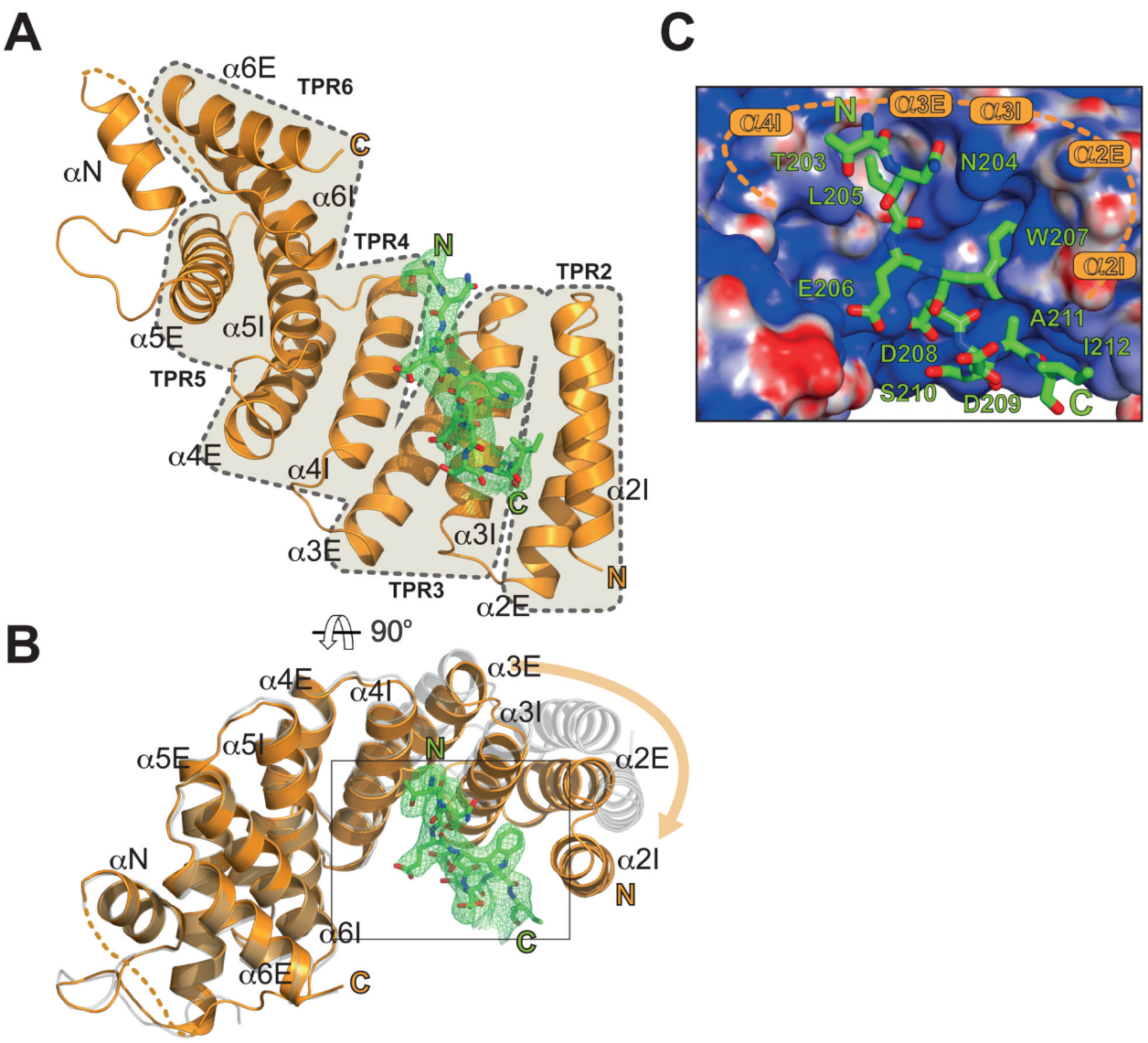

Figure 2.

Structure of the SKIP^{WD}-KLC2^{TPR} cargo complex. **(A,B)** Cartoon representations of the SKIP^{WD} motif (displayed as stick model in green) bound to KLC2^{TPR} domain (orange cartoon) in two orthogonal orientations. Simulated annealing (F_o-F_c) omit map for the W-acidic cargo motif is contoured at the 3σ level. Individual TPR repeats composed by helix-turn-helix elements (I and E for internal and external, respectively) are highlighted in A. A non-TPR helix (αN) is between TPR5 and TPR6. Panel B also shows the apo KLC2^{TPR} structure (grey transparent cartoon) with an orange arrow indicating the movement of the TPR2-3 region with respect to the common TPR4-6 reference frame. **(C)** Electrostatic potential surface representation of KLC2^{TPR} with its SKIP^{WD}-bound cargo. Positive and negative potential is shown in blue and red, respectively. Cargo recognition is achieved by a combination of charge complementarity and sequence specificity.

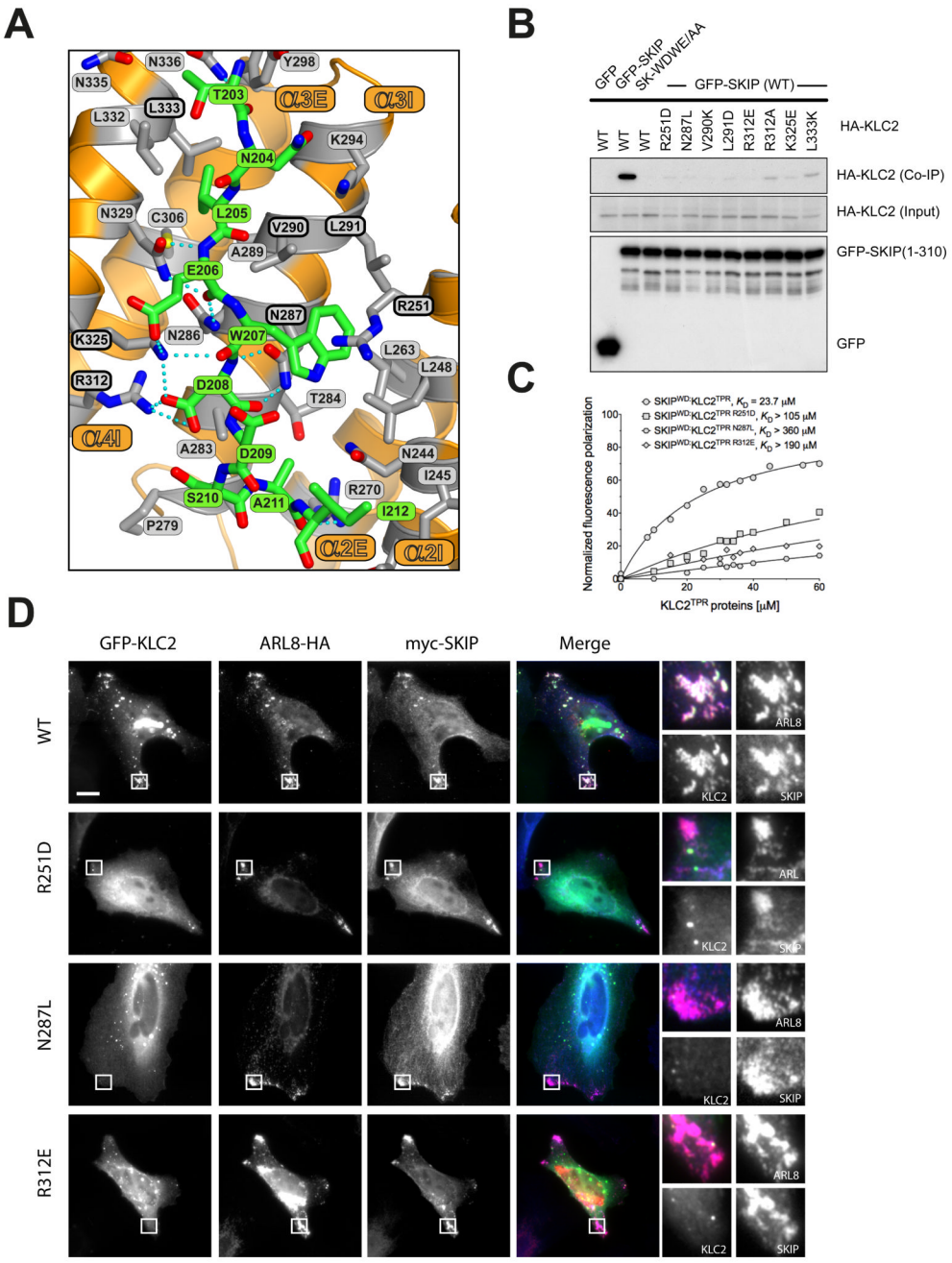

Figure 3.

The SKIP^{WD}-KLC2^{TPR} interface and the effect of KLC2^{TPR} mutations in cargo binding and cellular recruitment. **(A)** Details of the SKIP^{WD}:KLC2^{TPR} interface. KLC^{TRP} side-chains stabilizing the SKIP^{WD} cargo peptide (green) are shown as grey sticks emanating from the orange cartoon. Non-carbon elements are: nitrogen, blue; oxygen, red; sulfur, yellow. Hydrogen bonds are represented by dotted cyan lines. **(B)** Co-immunoprecipitation assay showing the effect of KLC2^{TPR} mutations at the SKIP^{WD}:KLC2^{TPR} interface on the interaction. **(C)** Fluorescence polarization measurements showing that R251D, N287L and R312E mutations in KLC2 dramatically reduce the affinity of the TPR domain for the

SKIP^{WD} peptide. K_D values reported here were calculated at 150 mM NaCl. **(D)** Replacement of key KLC2^{TPR} residues results in loss of GFP-KLC2 association with Arl8/SKIP positive lysosomal membranes. Scale bar shows 10μm. In merge panels, GFP-KLC2, Arl8 and SKIP are shown in green, red and blue respectively.

Europe PMC Funders Author Manuscripts